Office of Energy Efficiency & Renewable Energy

National Renewable Energy Laboratory

Innovation for Our Energy Future

Direct Comparison of Inverted and Non-Inverted Growths of GaInP Solar Cells

Preprint

M.A. Steiner, J.F. Geisz, R.C. Reedy, Jr., and S. Kurtz
National Renewable Energy Laboratory

Presented at the 33rd IEEE Photovoltaic Specialists Conference
San Diego, California
May 11–16, 2008

Conference Paper
NREL/CP-520-42559
May 2008

NREL is operated by Midwest Research Institute • Battelle Contract No. DE-AC36-99-GO10337

A DIRECT COMPARISON OF INVERTED AND NON-INVERTED GROWTHS OF GaInP SOLAR CELLS

Myles A. Steiner, John F. Geisz, Robert C. Reedy Jr. and Sarah Kurtz
National Renewable Energy Laboratory, Golden, CO

ABSTRACT

The inverted growth of III-V solar cells presents some specific challenges that are not present in regular, non-inverted growths. Because the highly doped top contact layer is grown first, followed by the lengthy high-temperature growth of the remainder of the structure, there is ample time for the dopants in the contact layer to diffuse away. This leads to an increase in the contact resistance to the top layer, and a corresponding drop in voltage. The diffusion of dopants in other layers is similarly altered with respect to the non-inverted configuration because of the change in growth sequence. We compare the dopant profiles of inverted and non-inverted structures by using secondary ion mass spectroscopy and correlate the results with the observed performance of the devices. We also describe a technique for growing a GaInAsN contact layer in the inverted configuration and show that it achieves a specific contact resistance comparable to what is normally observed in non-inverted cells.

INTRODUCTION

Inverted growth of III-V solar cells has become technologically important in the past five years. While the normal, upright configuration involves growing the thick base layer followed by the thinner emitter, in the inverted configuration the emitter is grown first. For an inverted multijunction cell, the top subcell is grown first, followed by the middle and bottom subcells, and after bonding the epilayers to a secondary handle such as silicon, the original substrate is removed to expose the top surface of the solar cell. One attractive feature of the inverted growth is that it may enable the recovery and reuse of the original substrate. Another feature is that it allows the bottom subcell to be grown mismatched with respect to the substrate. As demonstrated recently by Geisz *et al.* [1] in a triple junction GaInP/GaAs/GaInAs solar cell, enhanced performance may be achieved by lowering the bandgap of the bottom subcell, which involves growing those layers in compression. Even with graded layers to overcome the mismatch, in the upright configuration the additional dislocations in the bottom subcell may propagate up through the structure and adversely affect the top two junctions. In the inverted configuration, on the other hand, the unstrained top and middle subcells are grown lattice-matched and nearly defect-free, and then the transparent, graded layer and mismatched bottom subcell are grown. The cells in reference 1 demonstrated conversion efficiencies of 38.9% under 80 suns concentration.

The inverted growth process presents some challenges to the cell designer, however, which can severely limit the ultimate performance of the device. In a typical solar cell the emitter is thin and heavily doped, while the base is much thicker and more lightly doped (typical values may be 0.1 μm and $2x10^{18}$ cm^{-3} for the emitter, 3 μm and $1x10^{17}$ cm^{-3} for the base). The top contact layer is also thin and heavily doped to reduce the contact resistance. When grown inverted, the emitter, window and contact layers are subjected to a lengthy period at high-temperature as the remainder of the structure is grown, in what is essentially an annealing process. During this anneal, the dopants in these layers may diffuse into the more lightly doped layers of the structure. This can be a serious problem for the solar cell. Changes in the dopant levels lead to changes in the conductivities of the various layers, which may lead to increased series resistance and a lower fill factor, and consequently a lower operating power. Furthermore, because the depth and width of the junction are sensitive functions of the carrier concentrations, as the dopants diffuse away from their optimum positions the quantum efficiency will generally decrease and lead to a lower short circuit current; the open-circuit voltage may also be affected by the junction profile.

GROWTH DETAILS

In this paper, we explore directly the problem of atomic diffusion in inverted growths. We have fabricated sets of identical GaInP topcell structures, with some samples grown upright and others inverted, and characterized the atomic distributions in each. The samples were processed into solar cells to allow for a direct comparison of the performance and a measurement of the contact resistance. Our cells were grown in a vertical atmospheric pressure organometallic vapour phase epitaxy (OMVPE) reactor. Trimethylgallium, triethylgallium, trimethylindium, trimethylaluminum, arsine and phosphine precursors were used to synthesize the alloy epilayers. For the nitrogen-containing contact layers, dimethylhydrazine (DMH) was used as a precursor. Diethylzinc and hydrogen selenide were used as the dopants. The cells were grown at 650°C, except for the nitrogen-containing layers which were grown at 570°C [2]. Growth conditions are similar to those described elsewhere [1,3]. The layer structures for upright and inverted cells are shown in Figure 1. The nominal structure is the same between the upright and inverted samples,

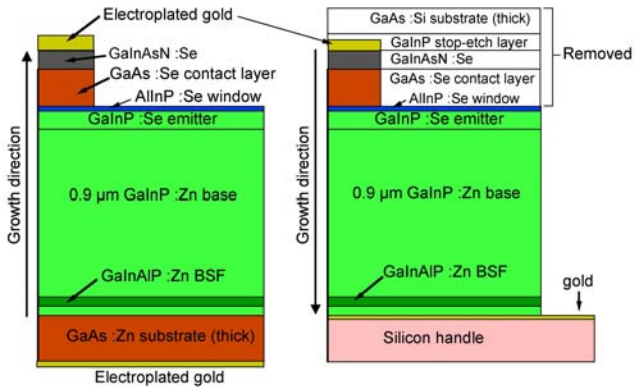

Figure 1 Layer structures for the upright (left) and inverted (right) cells. Note the difference in the growth directions. The light is incident from above in both diagrams.

and the corresponding layers were grown under the same conditions of temperature, rate and V/III ratio. All samples were contacted on top and bottom with electroplated gold [4]. After growth in the inverted configuration, the epilayers were bonded with epoxy to a silicon handle and the original GaAs substrate was removed. For the final, processed configurations, the only external difference between the two sets of samples is that in the upright samples the bottom contact is made through the doped substrate while in the inverted sample the bottom contact is made directly behind the cell, as shown in Figure 1.

SOLAR CELL CHARACTERISTICS

Figure 2 shows the current-density–voltage characteristics and internal quantum efficiencies for five different cells whose properties are listed in Table 1. The JV curves were measured on an XT-10 solar simulator using a GaInP reference cell calibrated for the lowAOD direct spectrum. The reflectance was measured simultaneously with the QE, using a calibrated photodiode. The growth process and doping levels for cells 1A and 1B were optimized for an inverted configuration. This is reflected in the QE data where both the peak and the blue response are better in the inverted cell (red curve) as compared to the upright cell (green). Voc and the fill factor are also lower for 1B. The cells 1C, 1D and 1E were optimized for an upright configuration, and correspondingly the QE for the upright cell 1C (blue) is better than the inverted cells 1D (purple) and 1E (black). The JV curve 1D shows clear non-ideal behaviour which we attribute to the poor contact resistance of the top contact. 1E is identical to 1D except that the top contact includes GaInAsN, similar to 1A, and the JV curve for this cell does not exhibit the non-ideality. Voc and the fill factor for 1D and 1E are both lower than the respective values for 1C. The QE data show that the bandgaps of all five cells are indistinguishable to within measurement error. These data illustrate that the same recipe grown upright and inverted can lead to a difference in performance

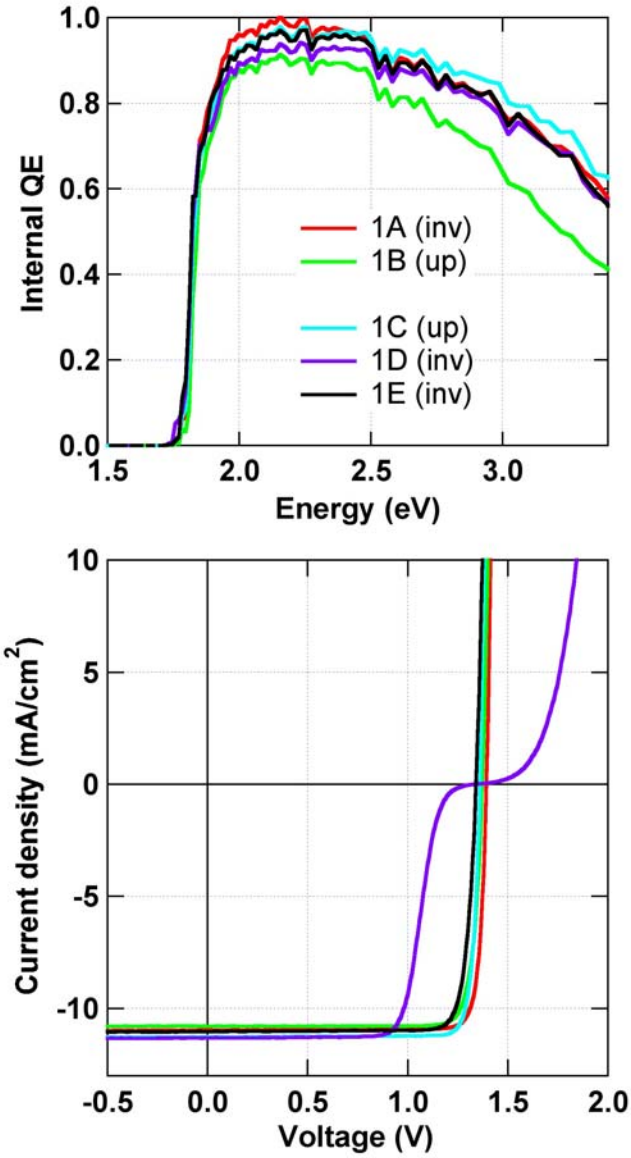

Figure 2 Internal QE (top) and JV (bottom) data for the five devices listed in Table 1. For the QE measurement, the reflectance was measured simultaneously with a calibrated photodiode. All data are unofficial.

between the cells.

Noteworthy in Table 1 are the differences in doping levels for corresponding cells. Both the emitter and base doping levels in the inverted 1A are significantly higher than the corresponding doping levels in the upright 1B. In the second set of cells the base doping level is higher in the upright cell 1C, while the emitter doping levels are comparable. The contact to 1D was found to be non-Ohmic.

We have analyzed the depth profiles of the cells in the first set with secondary ion mass spectroscopy (SIMS), using a Cs^+ source for the primary sputtering beam. Figure 3 shows the selenium, zinc and arsenic profiles for samples 1A and 1B. The concentrations of the

Sample		R_s (Ω/sqr)	R_c (mΩcm^2)	Emitter (10^{18} cm^{-3})	Base (10^{16} cm^{-3})	Voc (V)	Jsc (mA/cm^2)	FF (%)	Eff (%)
1A [MH560]	inv	326	0.088	-3.2	1.4	1.395	10.97	88.3	13.5
1B [MH581]	up	981	0.11	-0.98	0.36	1.372	10.79	86.8	12.9
1C [MH881]	up	600	0.50	-1.7	9.1	1.361	11.27	88.6	13.6
1D [MH891]	inv	--	--	--	4.5	1.306	11.31	68.7	10.2
1E [MH896]	inv	516	0.22	-2.1	3.1	1.340	11.03	86.3	12.8

Table 1 Measured parameters for five inverted and upright solar cells. The top two cells were optimized for an inverted growth, the bottom three cells were optimized for an upright growth. R_s is the emitter sheet resistance (determined from Hall); R_c is the specific contact resistance to the contact layer (TLM); The emitter and base dopings were determined from Hall and CV measurements. Most of the parameters for 1D were not measurable. The last sample, 1E was the same as 1D except that the top contact included GaInAsN.

selenium and zinc were calibrated by measuring ion implant standards to obtain relative sensitivity factors for the various alloys; the arsenic levels are shown as the measured count rates. The vertical lines give the approximate locations of the layer interfaces. The inverted sample was analyzed after it was processed, so that the growth direction is left-to-right, while the growth direction for the upright sample is right-to-left.

Comparing the selenium levels between the two samples, the concentration is nearly an order of magnitude higher in the Zn-doped base of the inverted sample. Because the selenium contact and window layers are grown before the base in the inverted sample, the dopant may diffuse out of these layers during the lengthy growth of the base. In the upright sample, on the other hand, there is relatively little time for diffusion out of the contact layers. The metallurgical concentrations in the contact layers are lower in the inverted sample, relative to the upright, despite the same growth conditions, which suggests a significant amount of out-diffusion.

The long selenium tail may also result from a memory effect in the growth reactor [5]. Selenium tends to coat the reactor walls and slowly desorb after the flow is turned off, leading to a gradually decreasing incorporation in the inverted sample. In the upright sample, the selenium flow is not turned on until after the base is fully grown. While the turn-on transient time of the selenium may affect the profile in the emitter, there is little opportunity for a memory effect to affect the profile in the base of the upright sample.

The zinc levels in the base are near the detection limit of the instrument, so it is difficult to determine if there is significant diffusion in the base. The zinc level is consistent with the concentrations extracted from capacitance-voltage measurements. In both cells there is no diffusion of zinc into the emitter and contact regions, though there does appear to be a small zinc tail at the back of the base of the upright cell, adjacent to the back-surface field (BSF). In this upright sample the BSF is effectively annealed during the growth of the base and some zinc diffusion might therefore be expected. As with the selenium in the inverted cell, it is impossible to determine whether the small zinc tail is primarily the result of diffusion or a memory-effect.

The junction in the inverted sample has formed significantly deeper than in the upright sample because of the elevated selenium level in the base region. However,

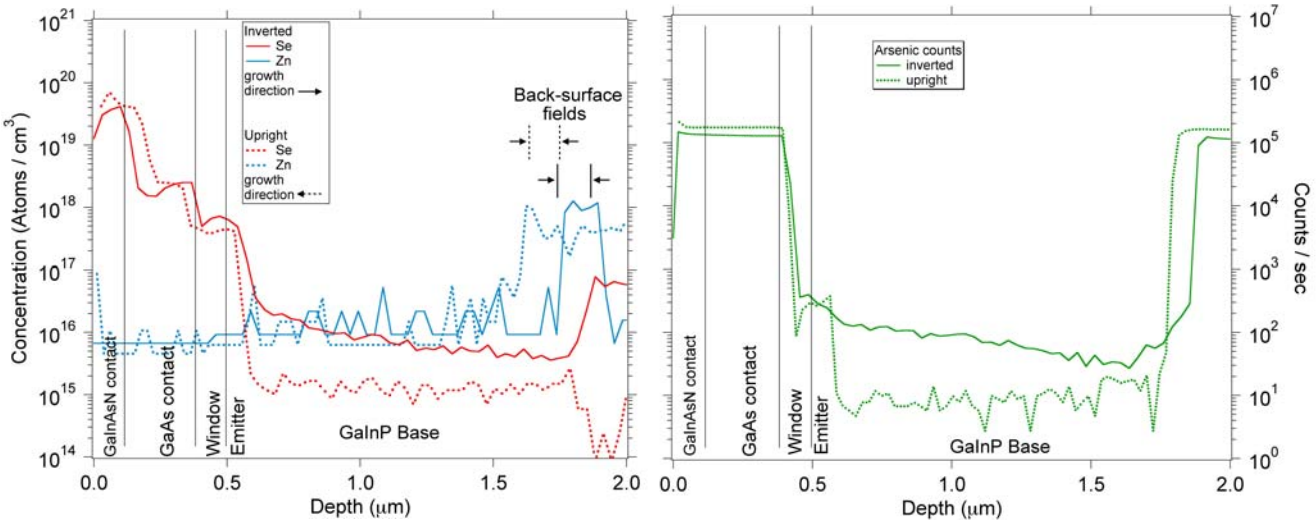

Figure 3 Secondary Ion Mass Spectroscopy (SIMS) profiles of the selenium and zinc concentration (left) and the arsenic count rate (right). The position of the back-surface field differs slightly between the two samples. For the upright cell (dashed lines) the growth direction is right-to-left, while for the inverted cell (solid lines) the growth is left-to-right.

the selenium doping level in the window layer of the upright sample is lower than in the inverted sample. The window layer is not explicitly doped during growth to avoid incorporating contaminants during the growth of the aluminum-containing layer, and instead relies on diffusion from the adjacent layers. It is not unexpected that the dopant concentration will be different between the upright and inverted cells. While the lower window doping of the upright cell increases the series resistance, as can be seen in Table 1, it also diminishes the front surface passivation. Therefore, despite the deeper junction, we observe a higher blue response in the quantum efficiency of the inverted sample in Figure 2. The SIMS data also show that the upright cell is approximately 0.15 μm thinner than the inverted cell, as evidenced by the shift in position of the back-surface field layer. While we cannot rule out an apparent shift in position due to non-uniformities in the growth, the shift is consistent with zinc diffusion during the remaining growth time. Since neither cell is optically thick the thinner upright cell absorbs less light, and therefore the red-response of the QE is found to be slightly lower in Figure 2.

We also observe elevated arsenic levels in the GaInP base region of the inverted sample, where no arsenic is expected. It is likely that the excess arsenic is a memory effect, coming from remnant molecules of the arsine precursor that have not been flushed from the system or are slowly desorbing from the reactor walls, though from the data we cannot conclusively rule out arsenic diffusion. It is not clear what effect, if any, the excess arsenic has on the cells' performance.

CONTACT LAYER

The selenium concentration in the contact layers is comparable in the two samples (1A and 1B), to within a factor of two, despite the difference in time at elevated temperatures. The measured specific contact resistances to these layers were similarly comparable, at 0.11 and 0.088 $m\Omega\text{-}cm^2$ for the upright and inverted structures, respectively. Contacting the top of the finished cell presents an especially important challenge in the inverted design, because any additional contact resistance translates directly into a loss in the fill factor at high concentration. In an upright cell, GaAs can be doped with selenium to a level of approximately 10^{19} cm^{-3}, to which excellent electrical contact is possible. In an inverted growth, however, where this layer is grown early in the structure, the selenium diffuses away from the contact layer and the contact resistance is found to be appreciably larger. The problem may be overcome by using a dilute nitride alloy (GaInAsN) that appears to bind the selenium dopants more tightly and raise the carrier concentration; in Figure 3, the selenium concentration in the GaInAsN alloy is approximately $5x10^{19}$ cm^{-3}, an order of magnitude higher than in the adjacent GaAs layers. To investigate this phenomenon more carefully, we grew a set of upright test structures consisting of 0.5 μm of GaInP and 0.1 μm of either a GaAs or a GaInAsN layer, all selenium-doped. In half of the samples, we grew an additional 2 μm of GaInP over 30 minutes to simulate the high temperature growth of the inverted top cell. The measured specific contact resistances (R_C) are listed in Table 2. Samples 2A and 2C simulate upright cells with the contacting layer grown last. Samples 2B and 2D simulate inverted cells with the contacting layer grown first. In the samples with only a GaAs contact, R_C increases by a factor of ~150 when the growth includes the high temperature anneal (2B). The bare GaInAsN alloy layer (2C) has comparable R_C to the GaAs layer (2A), while in the two "annealed" samples, the nitride layer (2D) performs better than the GaAs layer (2B) by a factor of 100. Indeed, R_C of sample 2D is nearly equal to that of sample 2A, despite the lengthy anneal. While the bandgap of the dilute nitride alloy is approximately 1.1 eV, it is etched away everywhere but under the contact metal and therefore does not absorb any incident light. This innovation was a key factor in the success of the inverted cell described in reference 1.

Sample	Contact layer	Contact resistance ($m\Omega\text{-}cm^2$)
2A [MH627]	GaAs, not annealed	0.013
2B [MH628]	GaAs, annealed	1.98
2C [MH629]	GaInAsN, not annealed	0.003
2D [MH623]	GaInAsN, annealed	0.020

Table 2 Specific contact resistances for electroplated gold contacts to the contact layer in the test structures. See the text for details.

SELENIUM DIFFUSION IN GaInAsN

We have attempted to understand more clearly the behaviour of the selenium in the GaInAsN alloy. Several authors [6,7] have demonstrated that the presence of nitrogen in the lattice leads to an elevated carrier concentration. Yu *et al.* attributed the increase to a pair of effects [6]: the nitrogen bonding leads to an anti-crossing of the conduction band, thereby splitting the band and effectively lowering the bandgap [6]. The reduced curvature of the lower conduction band leads to an increase in the electron effective mass and therefore an increase in the density of states at the conduction band edge.

We have conducted a set of experiments to investigate the diffusion of selenium in and out of GaInAsN. The concentration of nitrogen in the lattice was approximately one percent; the inclusion of two percent indium restored the alloy to the lattice-matched condition. We grew test structures as follows: on a chromium-doped GaAs substrate, we grew 2 μm of either undoped GaAs or undoped GaInAsN, followed by 0.1 μm of either Se:GaAs or Se:GaInAsN, followed by a thin layer of undoped GaInP. Four of the samples were then annealed for an additional 30 minutes at 650°C under a phosphine overpressure. This temperature corresponds to the nominal growth temperature of the middle and bottom subcells in the triple junction of reference 1. The remaining unannealed samples served as controls to evaluate the as-grown properties. The selenium-doped layers act as

Sample	Se:Source layer	Diffusion layer	Anneal?	n_{2D} (cm^{-2})	R_s (Ω/sqr)	R_c (mΩ-cm^2)	μ (cm^2/Vs)
3A [MH728]	GaAs	GaAs	No	-4.6 x10^{13}	146	0.28	932
3B [MH731]	GaAs	GaAs	Yes	-2.2	158	6.0	1740
3C [MH737]	GaAs	GaInAsN	No	-5.2	211	0.32	564
3D [MH740]	GaAs	GaInAsN	Yes	-3.4	325	5.6	564
3E [MH919]	GaInAsN	GaInAsN	No	-11.3	799	0.058	66
3F [MH741]	GaInAsN	GaInAsN	Yes	-6.0	949	0.23	109
3G [MH920]	GaInAsN	GaAs	No	-0.62	295	0.032	3410
3H [MH732]	GaInAsN	GaAs	Yes	-6.1	934	0.13	110

Table 3 Source and diffusion layers for study of selenium diffusion in GaInAsN. The sheet concentration n_{2D}, sheet resistance R_s and mobility μ were derived from a Hall measurement; the specific contact resistance R_c was derived from a TLM measurement.

source layers, and by growing them at the end there is limited possibility for diffusion before the explicit anneal, and no possibility for a turn-off memory effect to influence the dopant profile. The samples are identified in Table 3. Six of the eight samples were analyzed with SIMS in the same manner as described above, but with a slower sputtering rate; the data are shown in Figure 4. The concentrations of selenium were normalized with respect to a selenium-implanted GaAs calibrated reference sample [8].

The unannealed control sample 3A (blue) shows the extent of the selenium diffusion during the growth of the basic Se:GaAs/GaAs structure. 3B (purple) shows the additional diffusion in this structure after 30 minutes of annealing. The selenium has diffused to a greater depth, and the concentration in the source layer has been reduced. Comparing these samples with the unannealed control sample 3C (black) in which the diffusion layer is replaced with undoped GaInAsN indicates that the selenium has no inclination to diffuse into the nitride layer. Even upon annealing for 30 minutes (3D), no additional selenium is found to diffuse; the profiles of 3C and 3D (green) are nearly identical, and the concentrations in the source layer are nearly the same as in 3A.

All four of these samples show a selenium concentration of ~7x10^{18} cm^{-3} in the undoped GaInP cap layer. By contrast, the two samples 3F (yellow) and 3H (red) in which the source layer was GaInAsN show a lower concentration of ~2.8x10^{18} cm^{-3} in the cap layer. This is a larger relative difference than the relative difference in concentration in the source layer. It is likely that the initial incorporation of selenium into GaInAsN differs from the incorporation into GaAs under similar growth conditions, which accounts for the difference in source-layer concentrations between 3A and 3H, for example. The larger difference in concentrations in the GaInP layers must therefore be related to diffusion. This further suggests a strong binding of the selenium in the nitride layer, regardless of the composition of the adjacent layers.

Finally, comparing the annealed samples 3B (purple) and 3F (yellow) in which the alloy has the same composition throughout the structure (ie. the source and diffusion layers are the same), we find that in the case of GaAs the selenium readily diffuses, whereas in the case of GaInAsN the selenium does not diffuse at all.

The electrical characteristics of these samples are also displayed in Table 3. The GaInP cap layer was etched away before TLM and Hall patterns were fabricated. Because the SIMS data show that the selenium is largely confined to the doped source layer, we may consider the electrical measurements to be probes of the characteristics of mainly that layer. The contact resistance of the pairs 3A-3B and 3C-3D, with GaAs contact layers, increases substantially upon annealing, whereas the contact resistance for 3E-3F and 3G-3H which have a GaInAsN contact layer remain very low even after annealing. This trend is consistent with the earlier findings in Table 2, where the GaInAsN contact resistance was much more resilient under annealing than the GaAs contact resistance.

The mobilities of the annealed GaInAsN layers (except for 3G, as discussed below) are much lower than for the GaAs layers. As argued by Yu *et al.* [6], the reduced curvature of the conduction band leads to an increase in the effective mass, which leads to a decreased mobility. Table 3 also shows that the electron density is

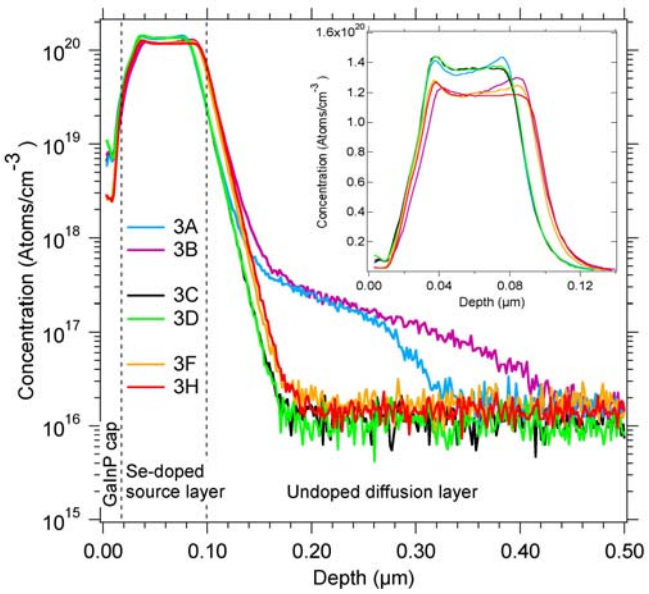

Figure 4 SIMS data for the GaInAsN test structures. The specifics for each of the different structures are described in Table 3. The inset shows the same data on a linear scale.

higher in the GaInAsN layers as compared to the GaAs layers, which would tend to lower the sheet resistance. Therefore the observed increase in the sheet resistance R_s in the GaInAsN layers is most likely dominated by the reduced mobility rather than the change in electron density.

The fact that the mobility changes by a factor of two for pairs 3A-3B and 3E-3F, whereas it remains constant for pairs 3C-3D suggests that in the former cases, where the alloy composition does not change, the current pathway probes the diffusion layer to the extent that selenium diffuses there. In the cases of 3C-3D, it appears that the current is confined to the GaAs source layer, in agreement with the SIMS data. It is not clear why the mobility of the unannealed sample 3G is so large, or the sheet density so low. It is possible that the GaInP cap layer was not completely etched away, though we would expect the contact resistance to be much higher if that were the case. It is also possible that the current pathway is more complex than simply going through the GaInAsN source layer, though this seems improbable given the data on sample 3H, and the similarities in R_s and μ between 3E, 3F and 3H.

The changes in electrical characteristics of the GaAs/GaAs samples correlate well with the SIMS data. On the contact side of the source layer (left side in Figure 4) the concentration of 3B is everywhere lower than 3A, and presumably so is the electrically active concentration. The SIMS data do not, however, readily explain the change in the GaAs/GaInAsN samples, for in that case the SIMS data are nearly identical. We speculate that while the metallurgical concentration of selenium remains unchanged despite the anneal, there may be a relative change in the interstitial-substitutional fraction of the selenium atoms [9]. It would be useful to measure the depth profile of the electrically active selenium, though at these high concentrations capacitance-voltage measurements are typically unreliable. Time-of-flight SIMS may yield higher resolution data at the contact interface, but that measurement remains a probe of the metallurgical rather than electrical concentration. A study of the bonding between selenium and the host atoms using Fourier transform infrared spectroscopy (FTIR) may yield useful information about the dominant mechanisms that inhibit the diffusion [9]. Nevertheless, we conclude from these data that (1) the diffusion of selenium is inhibited within the GaInAsN lattice, (2) there is little propensity for selenium to diffuse into or out of a GaInAsN lattice, and (3) the GaInAsN layer is significantly more resilient to changes in electrical characteristics during a high-temperature anneal than a bare GaAs layer.

SUMMARY

We have shown in this paper that there are significant differences in the depth profiles between similar structures grown upright and inverted. The concentrations of the dopants in the various layers may shift from their design concentrations because of diffusion during the lengthy growths. The top contact layer, grown early in the inverted device, is especially susceptible to changes in carrier concentration and specific contact resistance. These differences may affect the performance of the final solar cells. While the ability to grow cells in an inverted configuration may enable technological advancements in solar cell efficiency, it is imperative that the designer take proper consideration of the difference in the growth direction.

ACKNOWLEDGMENTS

The authors thank W. Olavarria, C. Kramer and M. Young for dedicated work growing and processing the devices. This work was supported by the U.S. Department of Energy under Contract No. DE-AC36-99GO10337 with the National Renewable Energy Laboratory.

REFERENCES / NOTES

[1] J.F. Geisz *et al.*, “High-efficiency GaInP/GaAs/InGaAs triple-junction solar cells grown inverted with a metamorphic bottom junction,” *Appl. Phys. Lett.*, **91**, 2007, pp. 023502 -023504.

[2] S.R. Kurtz, J.M. Olson, K.A. Bertness, K. Sinha, B. McMahon and S. Asher, *Proceedings of the 25th IEEE Photovoltaic Specialists Conference, Washington, DC* (IEEE, New York, 1996), p. 37.

[3] J.F Geisz *et al.*, “Photocurrent of 1 eV GaInNAs lattice-matched to GaAs,” *J. Cryst. Growth*, **195**, 1998, pp. 401-408.

[4] Electroplated gold contacts may give different results for the specific contact resistance from the evaporated contacts used in production.

[5] C.R. Lewis, M.J. Ludowise and W.T. Dietze, “H_2Se memory effects upon doping profiles in GaAs grown by MOCVD,” *J. Electron. Mater.*, **13**, 1984, pp.447-461.

[6] K.M Yu *et al.*, “Nitrogen-induced increase of the maximum electron concentration in group III-N-V alloys,” *Phys. Rev. B*, **61**, 2000, pp. 13337-13340.

[7] W. Shan *et al.*, “Band anticrossing in GaInNAs alloys,” *Phys. Rev. Lett.*, **82**, 1999, pp. 1221-1224.

[8] The Relative Sensitivity Factor (RSF) may differ slightly for this alloy of GaInAsN as compared to GaAs, but at 2% indium and ~1% nitrogen the difference is assumed to be small.

[9] S. Kurtz *et al.*, “Structural changes during annealing of GaInAsN,” *Appl. Phys. Lett.*, **78**, 2001, pp. 748-750.

REPORT DOCUMENTATION PAGE

Form Approved
OMB No. 0704-0188

PLEASE DO NOT RETURN YOUR FORM TO THE ABOVE ORGANIZATION.

1. REPORT DATE *(DD-MM-YYYY)*	2. REPORT TYPE	3. DATES COVERED *(From - To)*
May 2008	Conference Paper	11-16 May 2008

4. TITLE AND SUBTITLE
Direct Comparison of Inverted and Non-Inverted Growths of GaInP Solar Cells: Preprint

5a. CONTRACT NUMBER
DE-AC36-99-GO10337

5b. GRANT NUMBER

5c. PROGRAM ELEMENT NUMBER

6. AUTHOR(S)
M.A. Steiner, J.F. Geisz, R.C. Reedy, Jr., and S. Kurtz

5d. PROJECT NUMBER
NREL/CP-520-42559

5e. TASK NUMBER
PVA74401

5f. WORK UNIT NUMBER

7. PERFORMING ORGANIZATION NAME(S) AND ADDRESS(ES)
National Renewable Energy Laboratory
1617 Cole Blvd.
Golden, CO 80401-3393

8. PERFORMING ORGANIZATION REPORT NUMBER
NREL/CP-520-42559

9. SPONSORING/MONITORING AGENCY NAME(S) AND ADDRESS(ES)

10. SPONSOR/MONITOR'S ACRONYM(S)
NREL

11. SPONSORING/MONITORING AGENCY REPORT NUMBER

12. DISTRIBUTION AVAILABILITY STATEMENT
National Technical Information Service
U.S. Department of Commerce
5285 Port Royal Road
Springfield, VA 22161

13. SUPPLEMENTARY NOTES

14. ABSTRACT *(Maximum 200 Words)*

The inverted growth of III-V solar cells presents some specific challenges that are not present in regular, non-inverted growths. Because the highly doped top contact layer is grown first, followed by the lengthy high-temperature growth of the remainder of the structure, there is ample time for the dopants in the contact layer to diffuse away. This leads to an increase in the contact resistance to the top layer, and a corresponding drop in voltage. The diffusion of dopants in other layers is similarly altered with respect to the non-inverted configuration because of the change in growth sequence. We compare the dopant profiles of inverted and non-inverted structures by using secondary ion mass spectroscopy and correlate the results with the observed performance of the devices. We also describe a technique for growing a GaInAsN contact layer in the inverted configuration and show that it achieves a specific contact resistance comparable to what is normally observed in non-inverted cells.

15. SUBJECT TERMS
GaInP; PV; inverted configuration; contact layer; secondary ion mass spectroscopy; multijunction cell; open-circuit voltage; selenium diffsion; dopants;

16. SECURITY CLASSIFICATION OF:			17. LIMITATION OF ABSTRACT	18. NUMBER OF PAGES	19a. NAME OF RESPONSIBLE PERSON
a. REPORT	b. ABSTRACT	c. THIS PAGE			19b. TELEPHONE NUMBER (*Include area code*)
Unclassified	Unclassified	Unclassified	UL		